Journal of Structural Biology 209 (2020) 107439

Contents lists available at ScienceDirect

Journal of Structural Biology

journal homepage: www.elsevier.com/locate/yjsbi

Cryo-EM reveals an asymmetry in a novel single-ring viral chaperonin

Tatiana B. Stanishneva-Konovalova[a], Pavel I. Semenyuk[b], Lidia P. Kurochkina[b,*], Evgeny B. Pichkur[c], Alexander L. Vasilyev[c], Mikhail V. Kovalchuk[c], Mikhail P. Kirpichnikov[a,d], Olga S. Sokolova[a,*]

[a] Department of Bioengineering, Faculty of Biology, Lomonosov Moscow State University, Leninskie Gory 1, Bld 12, Moscow 119991, Russia
[b] Belozersky Research Institute of Physico-Chemical Biology, Lomonosov Moscow State University, Moscow 119234, Russia
[c] National Research Center "Kurchatov Institute", Moscow 123098, Russia
[d] Shemyakin-Ovchinnikov Institute of Bioorganic Chemistry, Russian Academy of Sciences, Moscow 117997, Russia

ARTICLE INFO

Keywords:
Chaperonin
Bacteriophage OBP
Cryo-EM
Homology modeling
Asymmetry
Nucleotide binding

ABSTRACT

Chaperonins are ubiquitously present protein complexes, which assist the proper folding of newly synthesized proteins and prevent aggregation of denatured proteins in an ATP-dependent manner. They are classified into group I (bacterial, mitochondrial, chloroplast chaperonins) and group II (archaeal and eukaryotic cytosolic variants). However, both of these groups do not include recently discovered viral chaperonins. Here, we solved the symmetry-free cryo-EM structures of a single-ring chaperonin encoded by the gene 246 of bacteriophage OBP *Pseudomonas fluorescens*, in the nucleotide-free, ATPγS-, and ADP-bound states, with resolutions of 4.3 Å, 5.0 Å, and 6 Å, respectively. The structure of OBP chaperonin reveals a unique subunit arrangement, with three pairs of subunits and one unpaired subunit. Each pair combines subunits in two possible conformations, differing in nucleotide-binding affinity. The binding of nucleotides results in the increase of subunits' conformational variability. Due to its unique structural and functional features, OBP chaperonin can represent a new group.

1. Introduction

The process of protein folding includes intermediate states where hydrophobic regions may become exposed and cause protein aggregation. Chaperonins, a family of barrel-shaped chaperones, assist the proper folding of newly synthesized proteins and protect stress denatured proteins from aggregation, in an ATP-dependent manner (Kawata, 1999, Reissmann et al., 2007). They usually form double-ring complexes with 7–9 subunits per ring, where each subunit consists of three domains: equatorial, intermediate and apical (Skjærven et al., 2015).

Equatorial domains form inter- and intra-ring contacts and contain ATP-binding pockets. ATP binding triggers the rigid body motion of domains relative to each other, which is enabled by two hinge points: the bottom equatorial-intermediate and the top intermediate-apical hinges. In group I chaperonins, these conformational changes are followed by the binding of the co-chaperonin to apical domains, which encapsulates the substrate protein inside the folding chamber. The order in which the processes in the two chambers occur is still debated: the 'bullet cycle' model states that folding chambers work alternately (Rye, 1999), while the 'football cycle' model assumes that they operate simultaneously (Sameshima et al., 2010; Taguchi, 2015). A recent study revealed that GroEL, a group I chaperonin, undergoes ring separation and exchange between complexes upon ATP-binding (Yan, 2018). In group II chaperonins, both rings appear to work simultaneously, and co-chaperonin functions are performed by the flexible protrusion helices from the apical domains. In contrast to chaperonins from group I, they often comprise different types of subunits, this leads to a higher degree of asymmetry. Despite the ongoing debates and a variety of unresolved questions, groups I and II are relatively well-studied, compared to the recently discovered virus-encoded chaperonins (Kurochkina, 2012; Semenyuk et al., 2015; Semenyuk et al., 2016).

Gene product (gp) 146 is the first functionally characterized viral chaperonin encoded by the genome of bacteriophage EL *Pseudomonas aeruginosa* (Kurochkina, 2012). Like *E. coli* GroEL, it is composed of double-stacked heptameric rings with a central cavity, but does not require a co-chaperonin for its activity. Three cryo-EM reconstructions revealed profoundly different conformations of EL chaperonin, depending on the bound nucleotide (Molugu, 2016). While EL chaperonin in the nucleotide-free and ATP-bound states possess double-ring morphology in closed and open conformations, respectively, its ADP-bound

* Corresponding authors at: Belozersky Research Institute of Physico-Chemical Biology and Department of Bioengineering, Faculty of Biology; Lomonosov Moscow State University, Moscow 119234, Russia.
E-mail addresses: lpk56@mail.ru (L.P. Kurochkina), sokolova@mail.bio.msu.ru (O.S. Sokolova).

https://doi.org/10.1016/j.jsb.2019.107439
Received 29 July 2019; Received in revised form 15 November 2019; Accepted 19 December 2019
Available online 21 December 2019
1047-8477/

state has a closed single-ring conformation.

The second most recently characterized viral chaperonin is gp246 of the bacteriophage OBP *Pseudomonas fluorescens* (Semenyuk et al., 2016). It possesses a 24% identity with EL chaperonin, and a 17% identity with GroEL from *E. coli*, at the amino-acid level. Recombinant OBP chaperonin suppresses thermal inactivation and aggregation of the substrate protein in an ATP-dependent manner, but, unexpectedly, was purified as a single ring.

Here, using cryo-EM and single particle analysis, we have obtained a three-dimensional reconstruction of the single-ring OBP chaperonin in the nucleotide-free state, at 4.3 Å resolution, its complex with an ADP at 6.5 Å, and, with a non-hydrolysable ATP analogue, ATPγS at 5.0 Å. All 3D structures possess intrinsic asymmetry. The interactions between the subunits in these asymmetric models can suggest the existence of a unique functional cycle.

2. Results

2.1. The symmetry-free structure of OBP chaperonin in the nucleotide-free state demonstrates a unique subunit arrangement

For cryo-EM, we used a purified sample of the recombinant OBP chaperonin that lacks any exogenous nucleotides (Supplementary figure 1). To obtain the 3D structure, we employed two widely used reconstruction tools: RELION-3.0 (Nakane, 2018) and cryoSPARC (Punjanji et al., 2017). We achieved an average resolution of 4.5 Å for the RELION-derived model (Supplementary figure 2) and 4.3 Å for the cryoSPARC-derived model (Supplementary figure 3). Both cryo-EM structures were solved as a single ring. The refined 3D reconstruction was 13 nm in width, at the equatorial part of the complex, and 7 nm in height (Fig. 1A, B). Compared to our negative stain structure of the same chaperonin (Semenyuk et al., 2015), the cryo-EM approach revealed a surprising degree of asymmetry (Fig. 1C and Supplementary figure 4), and a previously undescribed subunit arrangement.

At the level of equatorial domains, OBP chaperonin possesses a clear C7 symmetry and closely resembles the overall structure of the one ring of GroEL (Bartolucci et al., 2005; Xu et al., 1997). Interestingly, at the level of apical domains, the C7 symmetry diminishes and is replaced by a completely different pattern: three subunit pairs plus a single subunit. Fig. 1C shows slices through the equatorial and apical domains and their schematic representations. The subunits within each pair possess different conformations (here, alternating subunits were dubbed 'A' and 'B'). The unpaired subunit 'C' is less resolved in our asymmetrical 3D reconstruction, which implies its highly dynamic nature; it is likely to be in continuous motion between A and B conformations. For this reason, we decided to further focus on fully resolved subunits and build atomic models for A and B conformations.

A homology-based model of the gp246 subunit was built in MODELLER (Webb and Sali, 2016) using the GroEL crystal structure as a template (Protein Data Bank (PDB) ID code: 1aon). This initial model was separately fitted into the density maps of either A or B subunits, and refined in Phenix (Adams, 2010). Thereby, we obtained the atomic models for both A and B subunits (Fig. 2A) and docked them into the electron density of the heptamer (Fig. 2B).

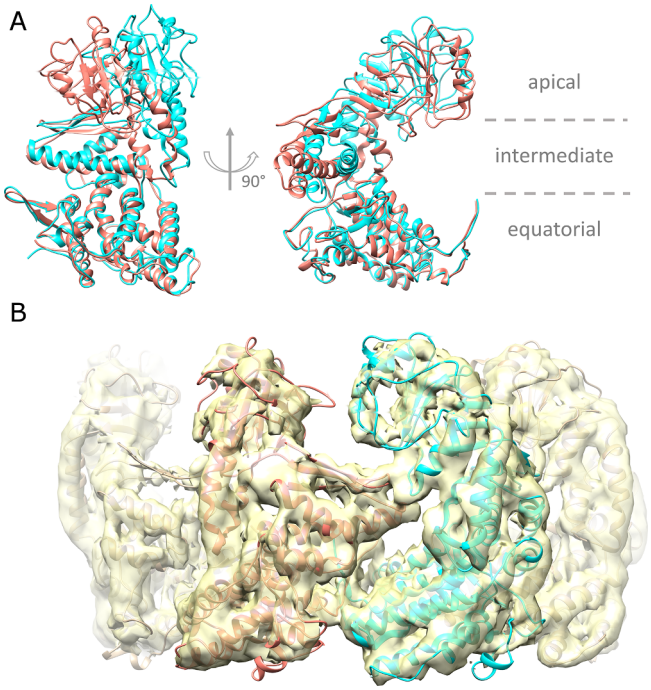

Fig. 2. The atomic models of A and B subunits of OBP chaperonin reveal the conformational difference. A. The alignment of A (pink) and B (cyan) subunits, at the level of their equatorial domains, shows the difference in the positions of intermediate and apical domains. B. Fitting the atomic models into the density map of a nucleotide-free state. Subunits are colored in accordance to the image in (A). (For interpretation of the references to colour in this figure legend, the reader is referred to the web version of this article.)

2.2. Comparison of the OBP chaperonin subunit structure with GroEL

According to sequence analysis, phage chaperonins seem to be closer to group I chaperonins (Semenyuk et al., 2016). Although GroEL and OBP chaperonin only have 17% sequence identity, alignment indicates the preservation of the nucleotide-binding site and hinge residues between the equatorial and intermediate domains in the OBP chaperonin (Supplementary figure 5). The situation is different with the inter-ring interface. In the GroEL subunits, two sites are responsible for inter-ring interactions: the first site is Lys105, Ala109, and the second – Arg452, Glu461, Val464 (Braig, 1994). The first site is also involved in transmitting the signal for ATP binding from one ring to the adjoining ring, providing the basis for negative inter-ring cooperativity (Ranson, 2006). According to our alignment, both sites are non-conserved in the gp246 sequence. These replacements may be the reason why we observe OBP chaperonin in our experiments only in the form of a single-

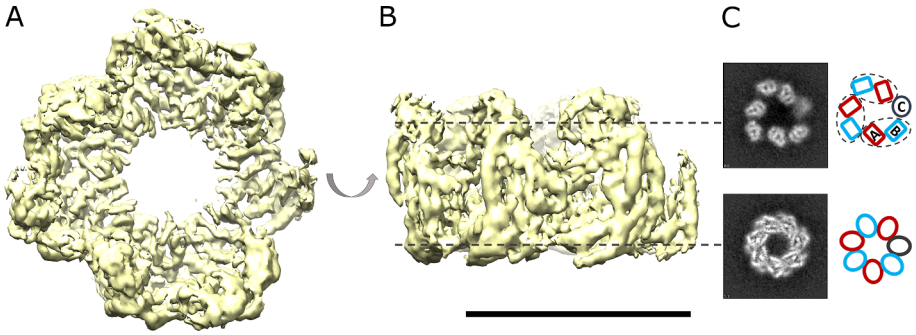

Fig. 1. Asymmetric density map of the nucleotide-free state of OBP chaperonin. A. Top view. B. Side view (bar size – 10 nm). C. Slices through the reconstruction at the level of apical (top panel) and the equatorial (bottom panel) domains, and their schematic representations (right). Subunits A, B, and C are colored red, blue, and black, respectively. Rectangles at the top depict apical domains, while dashed ellipses confine A-B subunit pairs. Ellipses at the bottom schematically depict equatorial domains of OBP chaperonin. (For interpretation of the references to colour in this figure legend, the reader is referred to the web version of this article.)

ring. To elaborate more on the asymmetry observed within the ring, we compared the atomic models of A and B subunits to the structures of the GroEL subunit in two conformational states (Clare, 2012).

In GroEL, the transition from a state with a lower affinity for ATP (T) to a state with a higher affinity (Rs1) is provided by a 35° tilting of the intermediate and apical domains around the bottom hinge. Upon this movement, the residue Asp398 of helix M of the intermediate domain comes closer to the ATP binding site (Xu et al., 1997). This transition happens simultaneously in all subunits of one ring (positive intra-ring cooperativity). Residues Pro137 and Gly410, which compose the bottom hinge between the equatorial and intermediate domains in GroEL (Xu et al., 1997), (Brocchieri and Karlin, 2000), are also conserved in OBP chaperonin. This indicates that the bottom hinge is present in OBP chaperonin, and it is likely providing the rotation of the apical-intermediate part relative to the equatorial domain.

The most remarkable differences in the structures of the single ring of GroEL and OBP chaperonin are observed in the apical domains; they are caused by the replacement of amino acids in the top hinge (Supplementary figure 6). In GroEL, the intermediate and apical domains are connected by highly conserved glycine residues Gly192 and Gly375, which provide transitions between different conformations within the functional cycle (Xu et al., 1997; Brocchieri and Karlin, 2000; Fei et al., 2013). In OBP chaperonin, the corresponded glycine residues are replaced by large polar residues Glu191 and Asn376, whose phi and psi values of torsion angles cannot provide efficient cis/trans switching (Hovmöller et al., 2002).

In GroEL, the concerted rotation of all apical domains leads to the opening/closing of the folding chamber during the ATP-dependent cycle. In OBP chaperonin, the isolated rotation of the apical-intermediate part resulted in the existence of two subunit conformations: namely, A and B (Fig. 2A). Apart from the apical domain's unique position, the conformation of the A subunit of OBP chaperonin in the apo-state is somewhat similar to the conformation of the T-state of GroEL (low affinity to nucleotides). At the same time, the B subunit conformation is more similar to the Rs1 (ATP-bound) state of GroEL (Clare, 2012) (Fig. 3). Thus, unlike GroEL, in the nucleotide-free state of OBP chaperonin, both conformations of subunits are represented simultaneously.

2.3. Structures of OBP chaperonin in nucleotide-bound states demonstrate the increased conformational variability of subunits

Like other chaperonins, OBP chaperonin functions using energy provided by ATP hydrolysis (Semenyuk et al., 2016). We investigated the interaction of OBP chaperonin with different nucleotides to determine the effect of nucleotide binding on its structure. First, we used the calorimetric titration of purified OBP chaperonin with ATP, ADP, and the non-hydrolysable ATP analogue – ATPγS (Supplementary figure 7). The latter is often used along with another analogue, AMP-PNP, to mimic the ATP-bound state of chaperonins (Boisvert et al., 1996; Zang, 2016).

The ITC curves for ATPγS and ADP are similar and are characterized by a low heat effect compared to ATP. Notably, all experimental data were best fit by the 'two sets of sites' model, indicating the existence of two sets of nucleotide-binding sites in the chaperonin subunits, which differ in binding constants and their corresponding heat effect. We proposed that these results reflect differences in the ability of A and B subunits to bind nucleotides. Apparently, the A subunit, where the relative position of the equatorial and intermediate domains is similar to the T state of GroEL, may have a lower affinity for nucleotides; the B subunit, in this part, on the contrary, is similar to the Rs1 state of GroEL, and, therefore, has a higher affinity for nucleotides. In all cases, the total apparent stoichiometry of binding is close to 7, which indicates that each subunit, despite its conformation, is capable of binding the nucleotide.

Next, we solved two asymmetrical 3D reconstructions: of the ATPγS-bound form, at a 5 Å resolution, and the ADP-bound form, at a 6.5 Å resolution (Fig. 4 and Supplementary figure 8). We confirmed the nucleotide binding by looking for additional densities in the nucleotide-binding pockets, using, as a reference, the equatorial domain of the previously reported crystal structure of GroEL-GroES in complex with ADP·AlFx (PDB ID code 1pcq) (Chaudhry, 2003). As expected, additional densities in the ATP-binding pockets were clearly present in all seven subunits of each nucleotide-bound form, and were absent in the nucleotide-free reconstruction (Supplementary figure 9).

Finally, we compared the conformations of the subunits in both nucleotide-bound structures (Fig. 4). Both ADP and ATPγS binding caused the increase of the conformational variability of subunits within the heptamer. As a result, more than one subunit adopted the 'C-subunit-like behavior', that is, a continuous motion between A and B conformations. To explore the mobility of subunits, we employed a 3D variability analysis tool implemented in cryoSPARC (Punjanji et al., 2017). The obtained movie demonstrated large conformational transitions of at least five subunits, wherein one of them was clearly changing its position between A and B (Movie 1). Since the top hinge in OBP chaperonin does not function properl as it does in GroEL, these conformational changes may only be provided by rotation in the bottom hinge. A replacement of one of the conserved glycine residues by isoleucine in the nucleotide-binding site of OBP chaperonin (colored blue in Supplementary figure 6A) may allow rotation in the bottom hinge, upon nucleotide binding.

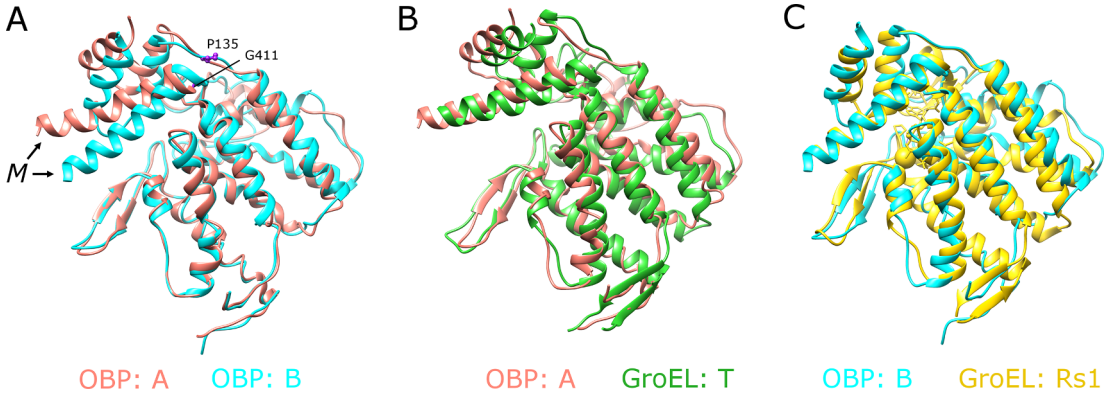

Fig. 3. Comparison of subunit conformations in OBP chaperonin and GroEL. Superimposition of A and B subunits of OBP chaperonin (A); The A subunit and the T state of GroEL (B) and the B subunit and the Rs1 state of GroEL (C). All structures are aligned by the equatorial domains. Only the equatorial domain and a part of the intermediate domain are shown for clarity. Helix M of the intermediate domain and residues composing the bottom hinge are indicated in (A).

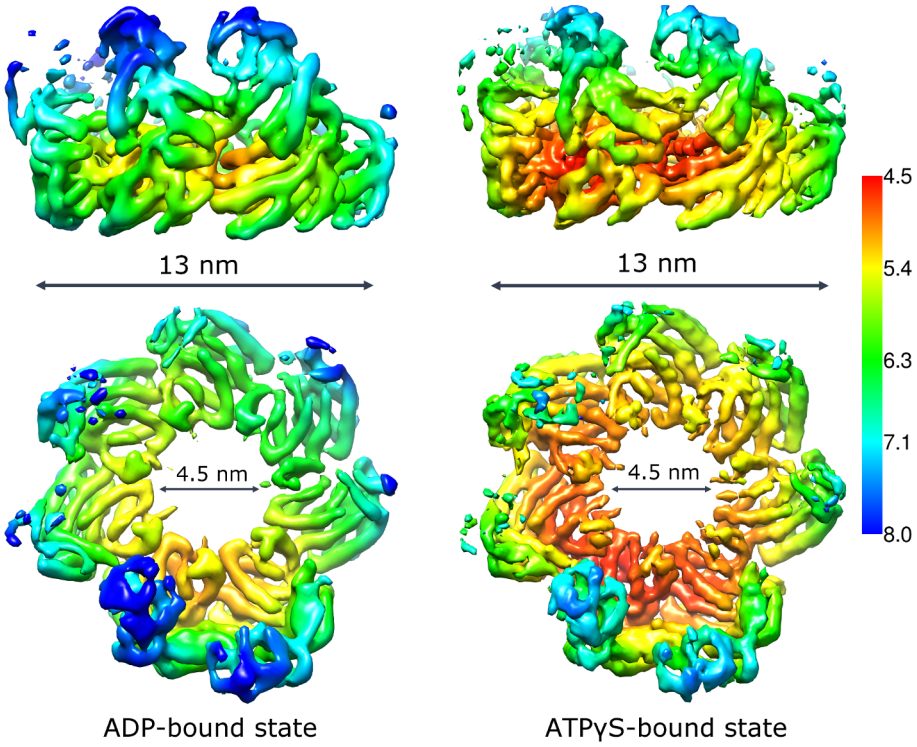

Fig. 4. Density maps of the nucleotide-bound states of OBP chaperonin. Side view (top panel) and top view (bottom panel) of ADP-bound and ATPγS-bound conformations of OBP chaperonin. Maps are colored according to the local resolution (in Å) estimated in Relion.

2.4. OBP chaperonin protects only small substrate proteins against aggregation

We concluded that, due to the disabled rotation of the apical domains and the presumable absence of a co-chaperonin, the cavity of the OBP chaperonin is most likely always open. So, how can the OBP chaperonin protect substrate proteins? To shed more light on this issue, we tested the anti-aggregation activity of purified OBP chaperonin on two proteins with different molecular masses: phage EL endolysin (gp188, 34 kDa), and a significantly larger protein – the rabbit tetrameric glyceraldehyde 3-phosphate dehydrogenase (GAPDH, 144 kDa). Note that, as it has previously been shown, the single-ring OBP exhibits anti-aggregation activity for substrate proteins only in the presence of ATP (Semenyuk et al., 2016), while the double-ring EL chaperonin and *E. coli* GroEL are able to passively (in the absence of ATP) protect substrates against aggregation through the formation of stable binary complexes (Kurochkina, 2012; Horwich et al., 2009). Interestingly, in the presence of ATP, the chaperone-like activity of OBP chaperonin for GAPDH was pronouncedly lower (Fig. 5A) than for endolysin (Fig. 5B), in contrast with phage EL chaperonin, which efficiently protects both enzymes against aggregation (Kurochkina, 2012; Semenyuk et al., 2017). Our results suggest that the OBP chaperonin is 'designed' to work with small substrates only, and not with large proteins.

3. Discussion

The bacteriophage-encoded OBP chaperonin was recently discovered and functionally characterized (Semenyuk et al., 2016). It possesses a structural resemblance to group I chaperonins, but, similarly to group II chaperonins and the recently characterized viral EL chaperonin (Kurochkina, 2012), no co-chaperonin was discovered by bioinformatic studies (Semenyuk et al., 2016; Molugu, 2016). In our previous study (Semenyuk et al., 2016), as well as here, the OBP chaperonin has been purified only in the form of a single ring. Hitherto, the

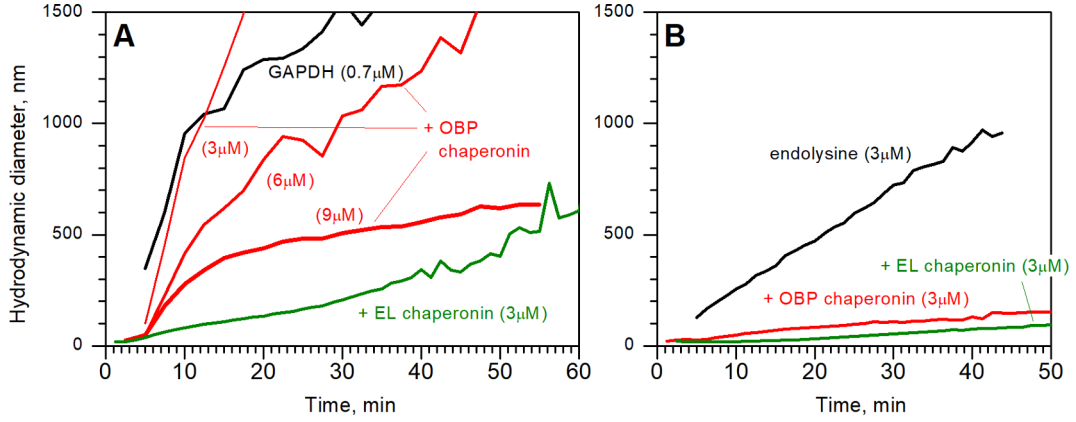

Fig. 5. Substrate binding of OBP chaperonin. The effect of OBP chaperonin (red curves) and EL chaperonin (green curves) on the thermal aggregation of GAPDH (A) and endolysin gp188 (B) at 45 °C. Black curves represent DLS trends of free substrate proteins. The ATP concentration was 1.2 mM, the protein concentration is indicated near each curve. Concentrations of substrate proteins, OBP chaperonin, and EL chaperonin were calculated for a monomer, heptamer, and tetradecamer, respectively. (For interpretation of the references to colour in this figure legend, the reader is referred to the web version of this article.)

single-ring conformation was reported for GroEL mutants (Kovács, 2010; Chen et al., 2006; Song et al., 2003), the apo-form of mitochondrial hsp60/10 chaperonin, and viral chaperonin EL in the ADP-bound state (Yan, 2018; Molugu, 2016; Nielsen et al., 1999; Nisemblat et al., 2015). Moreover, as was recently shown, the two heptameric rings can separate and exchange between complexes during the functional cycle of GroEL (Yan, 2018). To better understand the mechanism of OBP chaperonin functioning, we have solved four subnanometer resolution structures in the nucleotide-free and nucleotide-bound states, using cryo-EM.

We reveal the unique architecture of the nucleotide-free OBP chaperonin, which, despite being assembled from seven gp246 subunits, possesses a C7 rotational symmetry only at the level of equatorial domains. Thus, the equatorial parts of all four reconstructions possess the best resolution (Figs. 4, Supplementary figure 2 and Supplementary figure 3). At the level of intermediate and especially apical domains, the reconstruction lacks the rotational symmetry, but is organized as three pairs of subunits (A and B) plus one unpaired highly flexible subunit (C) instead (Fig. 1). Such conformational variability of subunits is enabled only by the bottom hinge, which connects the equatorial and intermediate domains. In group I chaperonins, all subunits undergo conformational changes in a concerted manner upon nucleotide binding (Horwich, 2011). This combined movement is lacking in the case of OBP chaperonin, due to the structural heterogeneity of its subunits. In this sense, OBP chaperonin is somewhat similar to group II chaperonins that are composed of different subunits. Yet, according to bioinformatics analysis, phage chaperonins have descended from group I chaperonins; therefore, we performed a structural and sequence comparison of OBP chaperonin to the most well-studied representative of group I: GroEL of *E. coli*. Although the equatorial domains of both chaperonins share an overall structure, the residues responsible for inter-ring interactions in GroEL are not conserved in OBP chaperonin, which could explain the observed single-ring conformation of the latter in our experiments. Another striking difference is caused by replacements in the top hinge, connecting the intermediate and apical domains. Amino acids Gly192 and Gly375, which in GroEL can switch between cis/trans conformations and allow the apical domain to rotate relative to the intermediate, are replaced by Glu191 and Asn376, respectively, in OBP chaperonin. In addition, Lys207 in GroEL is replaced by Ala206 in OBP chaperonin. Thus, salt bridges playing a key role in GroEL are most likely absent in the nucleotide-free state of OBP chaperonin. Instead, a new set of inter-subunit salt bridges appears. Although the resolution in the upper part of the complex does not allow for clear side chain identification, based on the proximity of the corresponding residues, we can assume the formation of several salt bridges. The molecular modeling unravels the following salt bridges that presumably connect the intermediate domain of the A subunit and the apical domain of the B subunit within each pair: Glu185 – Arg227, Lys187 – Glu256, and Lys381 – Glu254 (Fig. 6). Such interactions were not observed between subunits from adjacent pairs. As a result, the apical domains possess unique orientations (A and B subunits). This leads to the formation of alternating sets of inter-subunit salt bridges, and underlies the asymmetric pattern observed in the upper part of the complex.

Considering all of the above-mentioned special features of OBP chaperonin, one may expect that the effects of nucleotide binding would substantially differ from those observed for GroEL. Indeed, in both of the presently obtained nucleotide-bound structures of OBP chaperonin (Fig. 4), only one pair of subunits was clearly resolved. This conformation is, apparently, caused by the partial breakage of the inter-subunit salt bridges. Importantly, we observed the presence of an additional density in the ATP-binding pockets of all seven subunits, including the one pair that was fully resolved in our models. Thus, nucleotide binding may simplify switching between A and B conformations of neighboring subunits, but does not exclude the possibility of the A-B pair formation.

As a result, despite some similarities with the members of group I and group II, OBP chaperonin possesses a number of unique structural features. Our results imply that it may implement a novel functional cycle through the single-ring conformation. Nucleotide binding increases the conformational variability of subunits (Movie 1, Fig. 7), which is likely to affect substrate binding and folding. Another important feature is the disabled rotation of the apical domains, which would not allow for the chamber closure mechanism described for GroEL. We demonstrated previously that OBP chaperonin can protect substrate proteins against aggregation without a co-chaperonin, but only in the presence of ATP. Here, we show that this activity is much better manifested for a small 34 kDa endolysin than for a larger 144 kDa protein GAPDH. Whether the OBP chaperonin structure is somehow tailored for interactions with specific OBP phage proteins or not remains to be elucidated.

Finally, we speculated that, while the origin of phage chaperonins is clearly the group I chaperonin (Semenyuk et al., 2016), in an ancestor phage, our chaperonin was faced with a general problem: namely, the lack of a co-chaperonin. Thereby, in the course of evolution, OBP chaperonin obtained a unique asymmetric structure that provided specific interactions with substrate proteins. Noteworthy, the already known and predicted viral chaperonins are an extremely diverse group, and, probably, each member of this group fixed this problem separately, and, therefore, has its own unique features. Thus, our results open an exciting topic for the future research of viral chaperonins.

4. Methods

4.1. Expression and purification of recombinant gp246

Gene 246, cloned into plasmids under the control of the phage T7

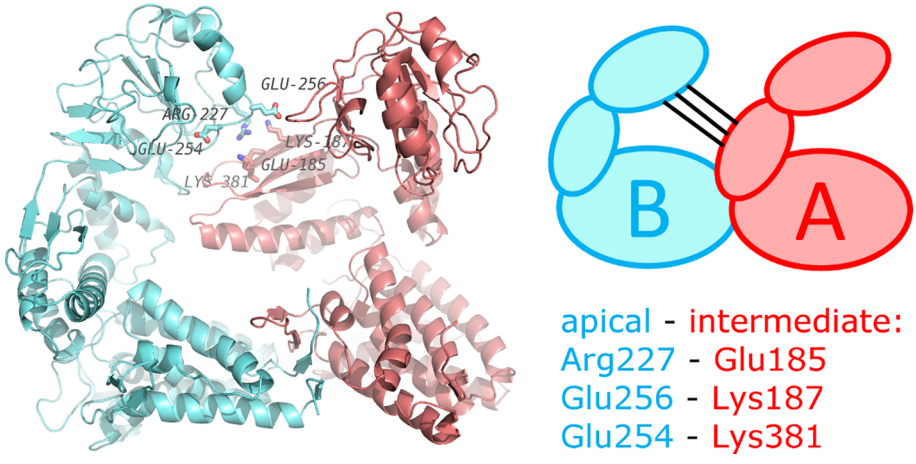

Fig. 6. Presumable inter-subunit contacts in OBP chaperonin. One pair of subunits, as seen from the central part of the complex (left), and its schematic representation (right). Amino acids forming salt bridges between A (pink) and B (cyan) subunits are indicated. (For interpretation of the references to colour in this figure legend, the reader is referred to the web version of this article.)

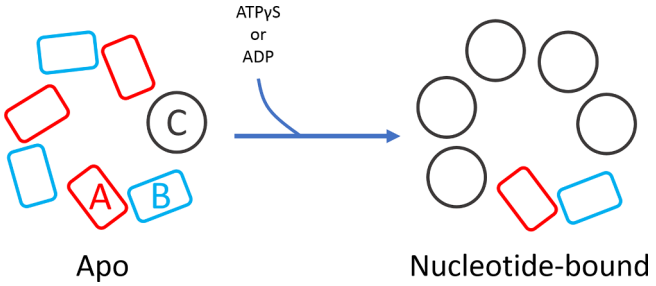

Fig. 7. Nucleotide-induced transitions of OBP chaperonin. In the apo-form, OBP chaperonin has a unique subunit arrangement, with three pairs of subunits (subunit conformations A and B are shown as red and blue rectangles, respectively) and one dynamic subunit C (grey circle). Upon nucleotide binding, more subunits became dynamic, each time leaving one pair of A-B subunits static. (For interpretation of the references to colour in this figure legend, the reader is referred to the web version of this article.)

promoter, was expressed in *E. coli* BL21(DE3), as previously described (Studier et al., 1990). Briefly, the recombinant bacteria were grown in a large volume of medium at 37 °C, until the A_{600} reached 0.7, induced with 1 mM isopropyl-β-D-thiogalactopyranoside (IPTG), and grown further for 3.5 h, at 25 °C. Cells were harvested, resuspended into 50 mM Tris-HCl (pH 7.5), sonicated using a Virsonic 100 disintegrator (Vertis, USA), and centrifuged (13000 g) to remove debris.

Nucleic acids were precipitated by adding 1/10 vol of 30% (w/v) streptomycin sulfate solution to a supernatant, followed by centrifugation. The recombinant protein was precipitated from the supernatant by the addition of a saturated ammonium sulfate to the final concentration of 30% (w/v). The protein precipitate was pelleted by centrifugation, dissolved in 50 mM Tris-HCl (pH 7.5) containing 100 mM NaCl, and fractionated on a Q-Sepharose column (Bio-Rad Laboratories) in a linear gradient from 0.1 to 0.5 M NaCl, in the same buffer. Protein fractions were analyzed by SDS-PAGE (Laemmli, 1970) (Supplementary figure 1A,B). Fractions containing pure protein were pooled and concentrated using an Amicon 100 ultrafiltration device (molecular-mass cut-off 100,000 Da; Millipore), and repeatedly washed with buffer, containing 50 mM Tris-HCl (pH 7.5), 10 mM $MgCl_2$, and 100 mM KCl. The homogeneity of the sample was estimated by size-exclusion chromatography on a Superose-6 column (Supplementary figure 1C). The gp246 concentration was determined spectrophotometrically at 280 nm, using a theoretical absorption coefficient of 50435 $M^{-1}{\cdot}cm^{-1}$.

4.2. Cryo-EM data collection

Nucleotide-free gp246 samples were diluted to a final concentration of 2.5 mg/ml, in a buffer containing 50 mM Tris-HCl (pH 7.5), 100 mM KCl, 10 mM $MgCl_2$. Nucleotide-bound samples were prepared by incubation of 2.5 mg/ml gp246 with 2 mM of either ADP or a non-hydrolysable analogue of ATP, ATPγS (Sigma) for 30 min, at RT. 3.0 μl of each sample was applied to the glow discharged in air grids (R1.2/1.3, Quantifoil) and plunge-frozen using the Vitrobot Mark IV, at 100% humidity and 4.5 °C. A total of 4017 movies for nucleotide-free gp246, 2572 movies for ADP-bound, and 2685 movies for ATPγS-bound samples were collected in automated data acquisition mode using the cryo-TEM Titan Krios (ThermoFisher Scientific), equipped with a XFEG-electron source and a direct electron detector Falcon II, at 300 kV accelerating voltage and 75000x magnification, resulting in a 0.86-Å pixel size. Each movie stack contained 10 (38 for apo-gp246) frames; an electron flux between ~60 and ~70 e/Å^2 (~100 e/Å^2 for apo-gp246) was used.

4.3. Image processing and 3D reconstruction

For the nucleotide-free structure, 3843 movie stacks were selected and subjected to motion-correction in MotionCorr2 (Zheng, 2017). Contrast transfer function parameters were estimated in CTFFIND (Mindell and Grigorieff, 2003). Further processing steps were done in Relion-3.0 (Nakane, 2018), and in cryoSPARC (Punjanji et al., 2017). After 3D classification, 127,180 particles were left for model refinement in RELION-3.0 (Nakane, 2018) with no symmetry applied. The final resolution of the structure was estimated to be 4.5 Å, based on the gold-standard Fourier shell correlation at 0.143 (Supplementary figure 2). The same dataset was reprocessed in cryoSPARC, using particles picked in Warp. After several rounds of 2D classification and 3D classification, 45,692 particles were used for refinement in cryoSPARC (Punjanji et al., 2017), that gave a resolution of 4.3 Å (Supplementary figure 3).

For ADP- and ATPγS-bound samples, 2017 and 2470 micrograph stacks were processed, respectively. The final refinement was accomplished in RELION-3.0. For ADP-bound reconstruction, 75,955 particles were included in the final refinement, resulting in a 3D reconstruction, at a 6.5 Å resolution; for the ATPγS-bound structure, 114,683 particles were used, and the achieved resolution was 5 Å (Supplementary figure 8). Principal component analysis of structural heterogeneity was performed in cryoSPARC (Punjanji et al., 2017) with three Eigen vectors and the low pass filter set to 6.5 Å.

4.4. Homology model building and optimization

A sequence of gp246 was obtained from the OBP phage genome deposited in GenBank under the accession code JN627160 (Cornelissen, 2012). The search for templates, model building and optimization was performed in MODELLER (Webb and Sali, 2016). The structure of a GroEL subunit (accession code in Protein Data Bank: 1aon) was chosen as a template. The homology-based model was initially fit as a rigid body into a density map of a single subunit using UCSF Chimera (Pettersen, 2004), and then subjected to flexible fitting in Direx (Schröder et al., 2007). For a nucleotide-free state, atomic models of two subunit conformations were replicated and rigid-body fit into the 4.5 Å resolution density map of the whole complex. The resulting atomic structure of OBP chaperonin was equilibrated in Phenix (Adams, 2010). The conformation of the A subunit was aligned with the apo state of GroEL (PDB ID code: 4hel), while the conformation of the B subunit was aligned with the Rs1-state of GroEL (PDB ID code: 4aaq).

4.5. Nucleotide binding assay

The interaction of OBP chaperonin with nucleotides (ATP, ADP, and ATPγS) was investigated using isothermal titration calorimetry (ITC) on a VP-ITC instrument (MicroCal) with a 1.4-ml cell, as previously described (Semenyuk et al., 2016). Experiments were carried out in 50 mM Tris-HCl (pH 7.5), 10 mM $MgCl_2$, and 100 mM KCl, at 25 °C. Titration experiments were performed by successive 10-μl injections of 110 μM ATP, 100 μM ADP or 94 μM ATPγS solution into the gp246 solution (0.7 mg/ml or 1.7 μM for heptamer), with 5 min intervals between injections. Binding isotherms were corrected by subtracting ligand dilution isotherms, determined by titrating nucleotide solutions into buffer. The 'two sets of sites' model was used for the fitting of data using MicroCal Origin 7.0 software. This model assumes the protein (here, a heptamer of OBP chaperonin) to have two different sets of binding sites. The sites in each set are equal to each other, but differ between the sets in thermodynamic parameters, i.e. association constant and enthalpy. A number of sites in each set represents a stoichiometry of the corresponding process.

4.6. Aggregation assay

The thermal aggregation of rabbit GAPDH and endolysin (gp 188 of

phage EL) in 50 mM Tris-HCl (pH 7.5), 100 mM KCl, 10 mM $MgCl_2$, at 45 °C, and in the absence and presence of chaperonin, were studied using dynamic light scattering (DLS) on a ZetaSizer NanoZS instrument (Malvern). The GAPDH was purified from rabbit muscle, as described elsewhere (Scopes and Stoter, 1982). Phage EL endolysin (gp188) was expressed in *E. coli* BL21(DE3) and purified, as described earlier (Kurochkina, 2012).

Data availability

Cryo-EM maps of OBP chaperonin in nucleotide-free, ADP-bound and ATPγS-bound states have been deposited to EMDB under accession numbers EMD-0204, EMD-0191 and EMD-0208, respectively. PDB ID has been obtained for the atomic model of the nucleotide-free state: 6HDD.

Author contribution

L.P.K., M.V.K., O.S.S. and M.P.K. designed the experiments. T.B.S.-K., P.I.S., E.B.P. and L.P.K. performed the experiments. A.L.V. provided key reagents. T.B.S.-K., P.I.S., E.B.P. and O.S.S. wrote the manuscript. All authors analyzed data and edited the manuscript.

Declaration of Competing Interest

The authors declare that they have no known competing financial interests or personal relationships that could have appeared to influence the work reported in this paper.

Acknowledgements

Authors would like to thank Dr. Evgeniya Pechnikova and Ms. Xi Wang for help with cryo-electron microscopy and data analysis and Mrs. Lisa Trifonova for proofreading the manuscript. This work was supported by the Russian Fund for Basic Research (#19-04-00605 to O.S.S. – cryo-EM and data processing; #18-04-01281 to L.P.K. – protein expression and purification, DLS and ITC studies). A.L.V. and E.B.P. acknowledge the support of the Russian Science Foundation (grant #18-41-06001). Cryo-EM sample preparation and data collection were performed using the equipment of the Probe and Electron Microscopy Resource Centre “Nanozond”, at the NRC “Kurchatov Institute”. This work has been carried out using computing resources of the federal collective usage center “Complex for Simulation and Data Processing for Mega-Science Facilities”, at the NRC “Kurchatov Institute”, http://ckp.nrcki.ru/.

Correspondence and requests for materials should be addressed to O.S.S. or L.P.K.

Appendix A. Supplementary data

Supplementary data to this article can be found online at https://doi.org/10.1016/j.jsb.2019.107439.

References

Kawata, Y., et al., 1999. Functional communications between the apical and equatorial domains of GroEL through the intermediate domain. Biochemistry 38, 15731–15740.
Reissmann, S., Parnot, C., Booth, C.R., Chiu, W., Frydman, J., 2007. Essential function of the built-in lid in the allosteric regulation of eukaryotic and archaeal chaperonins. Nat. Struct. Mol. Biol. 14, 432–440.
Skjærven, L., Cuellar, J., Martinez, A., Valpuesta, J.M., 2015. Dynamics, flexibility, and allostery in molecular chaperonins. FEBS Lett. 589, 2522–2532.
Rye, H.S., et al., 1999. GroEL-GroES cycling: ATP and nonnative polypeptide direct alternation of folding-active rings. Cell 97, 325–338.
Sameshima, T., Iizuka, R., Ueno, T., Funatsu, T., 2010. Denatured proteins facilitate the formation of the football shaped GroEL-(GroES)2 complex. Biochem. J. 427, 247–254.
Studier, F.W., Rosenberg, A.H., Dunn, J.J., Dubendorff, J.W., 1990. Use of T7 RNA polymerase to direct expression of cloned genes. Methods Enzymol. 185, 60–89.
Taguchi, H., 2015. Reaction cycle of chaperonin GroEL via symmetric ‘football’ intermediate. J. Mol. Biol. 427, 2912–2918.
Yan, X., et al., 2018. GroEL ring separation and exchange in the chaperonin reaction. Cell 172, 605–617.e11.
Kurochkina, L.P., et al., 2012. Expression and functional characterization of the first bacteriophage-encoded chaperonin. J. Virol. 86, 10103–10111.
Semenyuk, P.I., Orlov, V.N., Kurochkina, L.P., 2015. Effect of chaperonin encoded by gene 146 on thermal aggregation of lytic proteins of bacteriophage EL Pseudomonas aeruginosa. Biochemistry (Mosc.) 80, 172–179.
Semenyuk, P.I., Orlov, V.N., Sokolova, O.S., Kurochkina, L.P., 2016. New GroEL-like chaperonin of bacteriophage OBP P. fluorescens suppresses thermal protein aggregation in an ATP-dependent manner. Biochem. J. 2383–2393. https://doi.org/10.1042/BCJ20160367.
Molugu, S.K., et al., 2016. Ring separation highlights the protein-folding mechanism used by the phage EL-encoded chaperonin. Structure 24, 537–546.
Nakane, T., et al., 2018. New tools for automated high-resolution cryo-EM structure determination in RELION-3. Elife 7, 1–38.
Punjanji, A., Rubinstein, J.L., Fleet, D.A., Brubaker, M.A., 2017. cryoSPARC: algorithms for rapid unsupervised cryo-EM structure determination. Nat. Methods 14, 290–296.
Bartolucci, C., Lamba, D., Grazulis, S., Manakova, E., Heumann, H., 2005. Crystal structure of wild-type chaperonin GroEL. J. Mol. Biol. 354, 940–951.
Xu, Z., Horwich, A.L., Sigler, P.B., 1997. The crystal structure of the asymmetric GroEL-GroES-(ADP)7 chaperonin complex. Nature 388, 741–750.
Webb, B., Sali, A., 2016. Comparative protein structure modeling using MODELLER. Curr. Protoc. Protein Sci. 2016 2.9.1-2.9.37.
Adams, P.D., et al., 2010. PHENIX: A comprehensive Python-based system for macromolecular structure solution. Acta Crystallogr. Sect. D Biol. Crystallogr. 66, 213–221.
Braig, K., et al., 1994. The crystal structure of the bacterial chaperonin GroEL at 2.8 Å. Nature 371, 578–586.
Ranson, N.A., et al., 2006. Allosteric signalling of ATP hydrolysis in GroEL-GroES complexes. Nat. Struct. Mol. Biol. 13, 147–152.
Clare, D.K., et al., 2012. ATP-triggered conformational changes delineate substrate-binding and -folding mechanics of the GroEL chaperonin. Cell 149, 113–123.
Brocchieri, L., Karlin, S., 2000. Conservation among HSP60 sequences in relation to structure, function, and evolution. Protein Sci. 9, 476–486.
Fei, X., Yang, D., LaRonde-LeBlanc, N., Lorimer, G.H., 2013. Crystal structure of a GroEL-ADP complex in the relaxed allosteric state at 2.7 A resolution. Proc. Natl. Acad. Sci. 110, E2958–E2966.
Hovmöller, S., Zhou, T., Ohlson, T., 2002. Conformations of amino acids in proteins. Acta Crystallogr. Sect. D Biol. Crystallogr. 58, 768–776.
Boisvert, D.C., Wang, J., Otwinowski, Z., Horwich, A.L., Sigler, P.B., 1996. The 2.4 angstrom crystal structure of the bacterial chaperonin GroEL complexed with ATPgS. Nat. Struct. Biol. 3, 170–177.
Zang, Y., et al., 2016. Staggered ATP binding mechanism of eukaryotic chaperonin TRiC (CCT) revealed through high-resolution cryo-EM. Nat. Struct. Mol. Biol. 1–11. https://doi.org/10.1038/nsmb.3309.
Chaudhry, C., et al., 2003. Role of the gamma-phosphate of ATP in triggering protein folding by GroEL-GroES: function, structure and energetics. EMBO J. 22, 4877–4887.
Horwich, A.L., Apetri, A.C., Fenton, W.A., 2009. The GroEL/GroES cis cavity as a passive anti-aggregation device. FEBS Lett. 583, 2654–2662.
Semenyuk, P.I., Kurochkina, L.P., Gusev, N.B., Izumrudov, V.A., Muronetz, V.I., 2017. Chaperone-like activity of synthetic polyanions can be higher than the activity of natural chaperones at elevated temperature. Biochem. Biophys. Res. Commun. 489, 200–205.
Kovács, E., et al., 2010. Characterisation of a GroEL single-ring mutant that supports growth of escherichia coli and has GroES-dependent ATPase activity. J. Mol. Biol. 396, 1271–1283.
Chen, D.H., Song, J.L., Chuang, D.T., Chiu, W., Ludtke, S.J., 2006. An Expanded conformation of single-ring GroEL-GroES complex encapsulates an 86 kDa substrate. Structure 14, 1711–1722.
Song, J.L., Li, J., Huang, Y.S., Chuang, D.T., 2003. Encapsulation of an 86-kDa assembly intermediate inside the cavities of GroEL and its single-ring variant SR1 by GRoES. J. Biol. Chem. 278, 2515–2521.
Nielsen, K.L., McLennan, N., Masters, M., Cowan, N.J., 1999. A single-ring mitochondrial chaperonin (Hsp60-Hsp10) can substitute for GroEL-GroES in vivo. J. Bacteriol. 181, 5871–5875.
Nisemblat, S., Yaniv, O., Parnas, A., Frolow, F., Azem, A., 2015. Crystal structure of the human mitochondrial chaperonin symmetrical football complex. Proc. Natl. Acad. Sci. 112, 6044–6049.
Horwich, A.L., 2011. Protein folding in the cell: an inside story. Nat. Med. 17, 1211–1216.
Laemmli, U.K., 1970. Cleavage of structural proteins during the assembly of the head of bacteriophage T4. Nature 227, 680–685.
Zheng, S.Q., et al., 2017. MotionCor2: anisotropic correction of beam-induced motion for improved cryo-electron microscopy. Nat. Methods 4–5. https://doi.org/10.1038/nmeth.4193.
Mindell, J.A., Grigorieff, N., 2003. Accurate determination of local defocus and specimen tilt in electron microscopy. J. Struct. Biol. 142, 334–347.
Cornelissen, A., et al., 2012. Complete genome sequence of the giant virus OBP and comparative genome analysis of the diverse KZ-related phages. J. Virol. 86, 1844–1852.
Pettersen, E.F., et al., 2004. UCSF Chimera—a visualization system for exploratory research and analysis. J. Comput. Chem. 25, 1605–1612.
Schröder, G.F., Brunger, A.T., Levitt, M., 2007. Combining efficient conformational sampling with a deformable elastic network model facilitates structure refinement at low resolution. Structure 15, 1630–1641.
Scopes, R.K., Stoter, A., 1982. Purification of all glycolytic enzymes from one muscle extract. Methods Enzymol. 90, 479–490.